Astron. Astrophys. 349, 77–87 (1999)

ASTRONOMY AND ASTROPHYSICS

The HST view of FR I radio galaxies: evidence for non-thermal nuclear sources⋆

M. Chiaberge[1], **A. Capetti**[2], **and A. Celotti**[1]

[1] SISSA/ISAS, Via Beirut 2-4, I-34014 Trieste, Italy (chiab@sissa.it)
[2] Osservatorio Astronomico di Torino, Strada Osservatorio 20, I-10025 Pino Torinese, Italy

Received 27 January 1999 / Accepted 18 June 1999

Abstract. Unresolved nuclear sources are detected by the Hubble Space Telescope in the great majority of a complete sample of 33 FR I radio galaxies belonging to the 3CR catalogue.

The optical flux of these Central Compact Cores (CCC) shows a striking linear correlation with the radio core one over four decades, arguing for a non–thermal synchrotron origin of the CCC radiation. We also find evidence that this emission is anisotropic, which leads us to identify CCCs with the misoriented relativistic jet component which dominates in BL Lac objects. This interpretation is also supported by the similarity in the radio-to-optical and optical spectral indices.

The high rate of CCC detection (85%) suggests that a "standard" pc scale, geometrically thick torus is not present in low luminosity radio-galaxies. Thus the lack of broad lines in FR I cannot be attributed to obscuration.

CCC fluxes also represent upper limits to any thermal/disc emission. For a $10^9 M_\odot$ black hole, typical of FR I sources, these limits translate into a fraction as small as $\lesssim 10^{-7} - 10^{-5}$ of the Eddington luminosity.

Key words: galaxies: active – galaxies: elliptical and lenticular, cD – galaxies: jets – galaxies: nuclei

1. Introduction

Optical studies of radio galaxies are central for the understanding of the physics of their nuclei, by allowing to investigate the relationship between the environment/host galaxy and the occurrence of activity (e.g. the role of merging in the evolution of the nuclear fueling, Colina & De Juan 1995), the formation of jets, the 'schemes' unifying different classes of Active Galactic Nuclei (AGN) and in particular radio galaxies with object dominated by relativistic beamed emission (blazars) (e.g. Urry & Padovani 1995).

The original classification of radio galaxies by Fanaroff & Riley (1974) is based on a morphological criterion, i.e. edge darkened (FR I) vs edge brightened (FR II) radio structure. It was later discovered that this dichotomy corresponds to a (continuous) transition in total radio luminosity (at 178 MHz) which formally occurs at $L_{178} = 2 \times 10^{26}$ W Hz^{-1}. In this paper we focus on the properties of FR I radio galaxies, which represent the lower power objects.

From the optical point of view FR I are associated with elliptical galaxies, are generally found in regions of galaxy density higher than powerful radio sources (Zirbel 1997) and often show signs of interactions (Gonzales-Serrano et al., 1993). Their optical spectra are dominated by starlight with no evidence for a continuum component directly related to the active nucleus. In general faint narrow lines are present while no broad lines are detected (Morganti et al. 1992, Zirbel & Baum 1995).

Significant progress in the understanding of the inner structure of FR I has been obtained thanks to HST observations. Most importantly they revealed the presence of dusty or gaseous kpc scale disks in the nuclear regions of several FR I radio galaxies (Ford et al. 1994; Jaffe et al. 1993; De Koff et al. 1995; Van der Marel, & Van den Bosch 1998). The study of the dynamics of these disks provides one of the strongest pieces of evidence to date of the presence of supermassive black holes associated with the activity in galactic nuclei, with masses reaching $\sim 10^9 M_\odot$ (Harms et al. 1994, Macchetto et al. 1991, Ferrarese et al. 1996, Van der Marel & Van den Bosch 1998, Bower et al. 1998).

A further, newly discovered feature in FR I, which we will concentrate on, are faint, nuclear optical components, which might represent the (as yet) elusive emission associated with the AGN. Their study can be a powerful tool to directly compare the nuclear properties of FR I with those of other AGNs, such as BL Lac objects and powerful radio galaxies.

In fact, in the frame of the unification schemes of low luminosity radio loud AGN, FR I radio galaxies are believed to be the misaligned counterparts of BL Lacs (for a review, see Urry & Padovani 1995). In this scenario the non–thermal beamed emission from relativistic jets, which dominates in blazars, should also be present in radio galaxies although not amplified or even de-amplified. The possibility of directly detecting this component in the optical band thanks to the HST capabilities, has been explored by Capetti & Celotti (1999). They studied five radio

Send offprint requests to: M. Chiaberge

⋆ Based on observations with the NASA/ESA Hubble Space Telescope, obtained at the Space Telescope Science Institute, which is operated by AURA, Inc., under NASA contract NAS 5-26555 and by STScI grant GO-3594.01-91A

galaxies whose extended nuclear discs can be used as indicators of the radio source orientation. The ratio of the nuclear luminosities of FR I and BL Lacs with similar extended properties, shows a suggestive correlation with the orientation of the radio galaxies. This behavior is quantitatively consistent with a scenario in which also the FR I emission is dominated by the beamed radiation from a relativistic jet. Further, independent support to this interpretation comes from the rapid variability of the central source of M 87, the only object for which multi epoch HST data were available (Tsvetanov et al. 1998).

The role of obscuration in low luminosity radio galaxies is also still a matter of debate. Within the unification scheme for Seyfert galaxies, it is believed that in type 2 objects the Broad Line Region (BLR) and the nuclear continuum source are hidden by an absorbing, edge-on torus, while in Seyfert 1 our line of sight is within absorption-free visibility cones (Antonucci & Miller 1985). Similarly, a combination of obscuration and beaming is essential for the unification of powerful radio sources (Barthel 1989). However, although circumnuclear tori appear to be commonly associated with active galactic nuclei, there is as yet no evidence in favour of nuclear obscuring material in FR I (and this is not required by the FR I / BL Lac unified scheme, Urry & Padovani 1995). A search for H_2O megamasers (which have been successfully used to probe the dense molecular gas associated to the torus in Seyfert galaxies, Miyoshi et al. 1995, Braatz et al. 1996) in a sample of FR I galaxies gave negative results (Henkel et al. 1998).

In order to further and thoroughly investigate these issues, we consider a complete sample of 33 3CR radio galaxies, morphologically identified as FR I sources. For 32 of these, HST/WFPC2 images are available in the public archive. Most of the images were taken as part of the HST snapshot survey of the 3C radio source counterparts, and are already presented by Martel et al. (1999) (objects with $z < 0.1$) and by De Koff et al. (1996) (objects with $0.1 < z < 0.5$). Here we specifically focus on the origin of these unresolved nuclear sources, which we found to be present in most of the objects of the sample and to which we refer as Central Compact Cores (CCC).

The selection of the sample is presented and discussed in Sect. 2, while in Sect. 3 we describe the HST observations. In Sect. 4 and Sect. 5 we focus on the detection and origin of the CCC component, respectively and in Sect. 6 we discuss some of the consequences of our results. Our findings are summarized in the final Sect. 7.

2. The sample

Our sample comprises all radio galaxies belonging to the 3CR catalogue (Spinrad et al. 1985) and morphologically identified as FR I radio sources by Laing et al. (1983) and/or Zirbel & Baum 1995 (see Table 1).

However, the powerful but simple original morphological FR I/II classification has revealed to be often inadequate, as being somewhat subjective and sensibly depending on the quality, resolution and frequency of the available radio maps. Also, several radio sources show a complex morphology: for example signatures of FR I structures (such as extended plumes and tails) can be detected together with typical characteristics of FR II sources (narrow jets and hot spots) in sources which might represent transition FRI/II objects (see e.g. Parma et al. 1987, Capetti et al. 1995). Furthermore, even among the edge darkened radio galaxies, a large variety of structures is present, including wide and narrow angle tails, fat doubles and twin jet sources. Although all these objects are classified as FR I and share the common characteristic of a low total radio luminosity, it is far from obvious that they represent a well defined class.

Therefore, in order to establish possible differences among the optical properties of the various subclasses of FR I galaxies and also directly re-assess their radio morphology against erroneous or doubtful identifications, we searched the literature for recent radio maps of each object of our sample. The radio structure of at least four sources is peculiar, there are several transition FR I/II objects and each of the FR I morphological 'types' described above is represented in the sample. In view of this ambiguity of the simple morphological classification, in the following we will also consider separately objects below and above a total radio luminosity of $L_{178} = 2 \times 10^{26}$ W Hz^{-1}, i.e. the fiducial radio power separation between FR I and FR II. Two thirds of the sources of our sample lie below this value.

Having only excluded 3C 231 (M 82) from the original list, as it is in fact a well known starburst galaxy, the remaining radio galaxies constitute a complete, flux limited sample of 33 FR I sources. In Table 1 we report redshifts, radio fluxes and total luminosities as taken from the literature: redshifts span the range $z = 0.0037 - 0.29$, with a median value of $z = 0.03$, and total radio luminosities at 178 MHz are between $10^{23.7}$ and $10^{28.1}$ W Hz^{-1} ($H_0 = 75\,\mathrm{km\,s^{-1}}$ Mpc^{-1} and $q_0 = 0.5$ are adopted hereafter).

3. HST observations

HST observations are available in the public archive (up to July 1998) for 32 out of the 33 sources (only 3C 76.1 has not been observed). The HST images were taken using the Wide Field and Planetary Camera 2 (WFPC2). The pixel size of the Planetary Camera, in which the target is always located, is $0''.0455$ and the 800×800 pixels cover a field of view of $36'' \times 36''$. The whole sample was observed using the F702W filter as part of the HST snapshot survey of 3C radio galaxies (Martel et al. 1999, De Koff et al. 1996). For about half of the sources, additional archival images taken through narrow and broad filters are also available. The HST observations log is reported in Table 2.

The data have been processed through the PODPS (Post Observation Data Processing System) pipeline for bias removal and flat fielding (Biretta et al. 1995). Individual exposures in each filter were combined to remove cosmic rays events.

In Figs. 1, 2 we present the final broad band images of the innermost regions ($1.5''$ – $6''$) of our 32 radio galaxies. The most interesting feature which is present in the great majority of them, is indeed an unresolved central source.

Table 1. Summary of radio and optical data of the sample.

Name	Other name	Redshift z	F_c (5 GHz) mJy	ref.	F_t (178 MHz) Jy	L_t (178 MHz) W Hz^{-1}
3C 028		0.1952	<0.2	G88	16.3	26.94
3C 029	UGC 595	0.0448	93.0	M93	15.1	25.71
3C 031	NGC 383	0.0169	92.0	G88	16.8	24.93
3C 066B		0.0215	182.0	G88	24.6	25.30
3C 075		0.0232	39.0	M93	10.5	25.00
3C 76.1		0.0324	—		12.2	25.35
3C 078	NGC 1218	0.0288	964.0	M93	19.75	25.46
3C 083.1	NGC 1265	0.0251	21.0	R75	26.6	25.47
3C 084	NGC 1275	0.0176	42370.0	T96	40.5	25.32
3C 089		0.1386	49.0	Z95	20.2	26.76
3C 264	NGC 3862	0.0206	200.0	G88	26.0	25.29
3C 270	NGC 4261	0.0074	308.0	G88	55.45	24.73
3C 272.1	M 84	0.0037	180.0	G88	19.4	23.68
3C 274	M 87	0.0037	4000.0	G88	1050.0	25.42
3C 277.3	COMA A	0.0857	12.2	G88	9.0	26.03
3C 288		0.2460	30.0	G88	18.9	27.17
3C 293	UGC 8782	0.0452	100.0	G88	12.7	25.65
3C 296	NGC 5532	0.0237	77.0	G88	13.0	25.11
3C 305	IC 1065	0.0414	29.5	G88	15.7	25.66
3C 310		0.0540	80.0	G88	55.1	26.43
3C 314.1		0.1197	<1.0	G88	10.6	26.37
3C 315		0.1083	150.0	G88	17.8	26.51
3C 317	UGC 9799	0.0342	391.0	M93	47.3	25.98
3C 338	NGC 6166	0.0303	105.0	G88	46.9	25.87
3C 346		0.1620	220.0	G88	10.9	26.62
3C 348	Her A	0.1540	10.0	M93	350.0	28.09
3C 386		0.0170	14.	S78	23.9	25.09
3C 424		0.1270	18.	B92	14.0	26.54
3C 433		0.1016	5.	G88	56.2	26.96
3C 438		0.2900	17.0	Z95	46.3	27.68
3C 442	ARP 169	0.0262	2.0	G88	16.1	25.29
3C 449	UGC 12064	0.0181	37.0	G88	11.5	24.82
3C 465	NGC 7720	0.0301	270.0	G88	37.8	25.78

F_c and F_t are the core and total radio fluxes. In column 5 we report the references to the core fluxes. B92: Black et al. 1992, G88: Giovannini et al. 1988, L91: Leahy & Perley 1991, M93: Morganti et al. 1993, R75: Riley & Pooley 1975, T96: Taylor et al. 1996, Z95: Zirbel & Baum 1995, S78: Strom et al. 1978. The radio core flux of 3C 424 has been estimated from the contour map (observations at 8.3 GHz).

4. The Central Compact Cores

4.1. Identification of CCCs

While it is straightforward to identify unresolved sources when they are isolated, the situation is more complex when these are located at the center of a galaxy, superposed to a brightness distribution with large gradients and whose behaviour in the innermost regions cannot be extrapolated from its large scale structure with any degree of confidence.

We therefore adopted a simple operative approach: we derived the radial brightness profiles of the nuclear regions of all galaxies using the IRAF *RADPROF* task and measured the FWHM setting the background level at the intensity measured at a distance of $\sim$5 pixels ($\sim$0.23″) from the center. In 22 cases the measured FWHM is in the range 0.05″ – 0.08″, i.e. indicative of the presence of an unresolved source at the HST resolution.

In 5 cases, namely 3C 28, 3C 89, 3C 314.1, 3C 424 and 3C 438, the fitting procedure yields FWHM larger than $0.15''$. The behaviour of these sources is radically different from those in which a CCC is detected and therefore we believe that, even with this operative definition, no ambiguity exists on whether or not a central unresolved source is present.

The remaining 5 sources have complex nuclear morphologies. The central regions of 3C 75, 3C 293, 3C 305 and 3C 433 are covered by dust lanes. Bright compact knots are seen, but they are completely resolved and offset from the center of the galaxy. Conversely 3C 315 has a peculiar highly elongated structure, contrasting with the typical roundness of FR I host galaxies, and no central source is seen.

Table 2. Log of HST observations

Name	Filter	t_{exp} (s)	Date	Name	Filter	t_{exp} (s)	Date
3C 28	F702W	280	17/10/94	3C 277.3	F702W	560	16/03/94
3C 29	F702W	280	12/01/95		F555W	600	06/06/96
3C 31	F702W	280	19/01/95		FR680N	600	27/11/95
	FR680N	600	01/09/95	3C 288	F702W	280	30/04/95
3C 66B	F702W	280	18/03/94	3C 293	F702W	280	15/01/95
3C 75	F547M	900	10/03/97	3C 296	F702W	280	14/12/94
	F791W	750	10/03/97	3C 305	F702W	560	4/09/94
	F673N	2500	10/03/97	3C 310	F702W	280	12/09/94
3C 76.1	—	—	—-	3C 314.1	F702W	280	22/12/94
3C 78	F702W	280	17/08/94	3C 315	F702W	280	29/11/94
	F673N	600	07/08/95	3C 317	F814W	6500	10/08/97
	F555W	600	16/09/96		F555W	6200	10/08/97
3C 83.1	F702W	280	22/07/94	3C 338	F702W	280	09/09/94
	F673N	600	22/10/95		F673N	600	27/11/95
3C 84	F702W	560	31/03/94	3C 346	F702W	280	01/08/94
	F450W	200	16/11/95	3C 348	F702W	280	09/05/94
3C 89	F702W	280	02/07/94	3C 386	F702W	280	1/04/ 95
3C 264	F547M	900	19/05/96	3C 424	F702W	280	05/09/94
	F673N	2500	19/05/96	3C 433	F702W	280	26/04/95
	F791W	750	19/05/96	3C 438	F702W	300	15/12/94
3C 270	F791W	800	13/12/94	3C 442	F791W	280	29/12/94
	F547M	800	13/12/94		F673N	2500	20/04/96
3C 272.1	F814W	520	04/03/96		F547M	900	20/04/96
	F547M	1200	04/03/96	3C 449	F702W	280	06/08/94
	F658N	2600	04/03/96		FR680N	600	24/08/95
3C 274	F814W	30	03/02/95	3C 465	F702W	280	23/01/95
	F547M	30	03/02/95		F673N	600	23/08/95

4.2. CCC photometry

The F702W transmission curve covers the wavelength range 5900–8200 Å and thus, within our redshift range, includes the Hα and [N II] emission lines. To estimate the continuum emission of the CCC we therefore preferred, when possible, to use images obtained with the F814W or F791W filters which are relatively line-free spectral regions up to a redshift of 0.075.

We performed aperture photometry of the 22 CCCs, adopting the internal WFPC2 flux calibration, which is accurate to better than 5 per cent. However, the dominant photometric error is the determination of the background in regions of varying absorption and steep brightness gradients, especially for the faintest CCCs, resulting in a typical error of 10% to 20%. Narrow-band images were used, where available, to remove the line contamination from the F702W images. We found that the line contribution is typically 5 to 40 per cent of the total flux measured in the F702W filter, therefore even the uncorrected fluxes are (for our purposes) reliable estimates of the continuum level. Optical fluxes of the CCCs are given in Table 3.

HST images in two broad filters are available for 9 galaxies. However, only in 5 cases (3C 78, 3C 84, 3C 264, 3C 272.1, 3C 274) is the accuracy of the photometry sufficient to deduce reliable estimates of the optical slope. For the last three objects data were taken simultaneously in the two bands, which avoids uncertainties due to possible variability. Galactic extinction is significant (and we corrected for it) only in the case of 3C 84, for which $A_B = 0.7$. In 3C 272.1 we estimated, by comparing the F547M and the F814W images, that the extended nuclear dust lane produces an absorption of 1–2 mag in the V band. The derived spectral indices (corrected for reddening) are in the range $\alpha_o = 0.7$–1.3 ($F_\nu \propto \nu^{-\alpha}$).

For the galaxies only showing diffuse emission we set as upper limits the light excess of the central 3x3 pixels with respect to the surrounding galaxy background. For the complex sources no photometry was performed.

5. Origin of the Central Compact Cores

As already pointed out in the introduction, although the presence of nuclear optical emission associated with the active nuclei of FR I radio galaxies is not a surprising feature, it is important to investigate its origin. With this aim we now explore possible (cor-)relations between the CCC flux/luminosity and other observed properties.

No trend is found between CCC luminosities and total radio power or absolute visual magnitude of the host galaxy. Conversely, the CCCs emission bears a clear connection with the radio core. In Fig. 3 we plot the optical flux of the CCCs F_o versus the core radio flux F_r (at 5 GHz): a clear trend is visible.

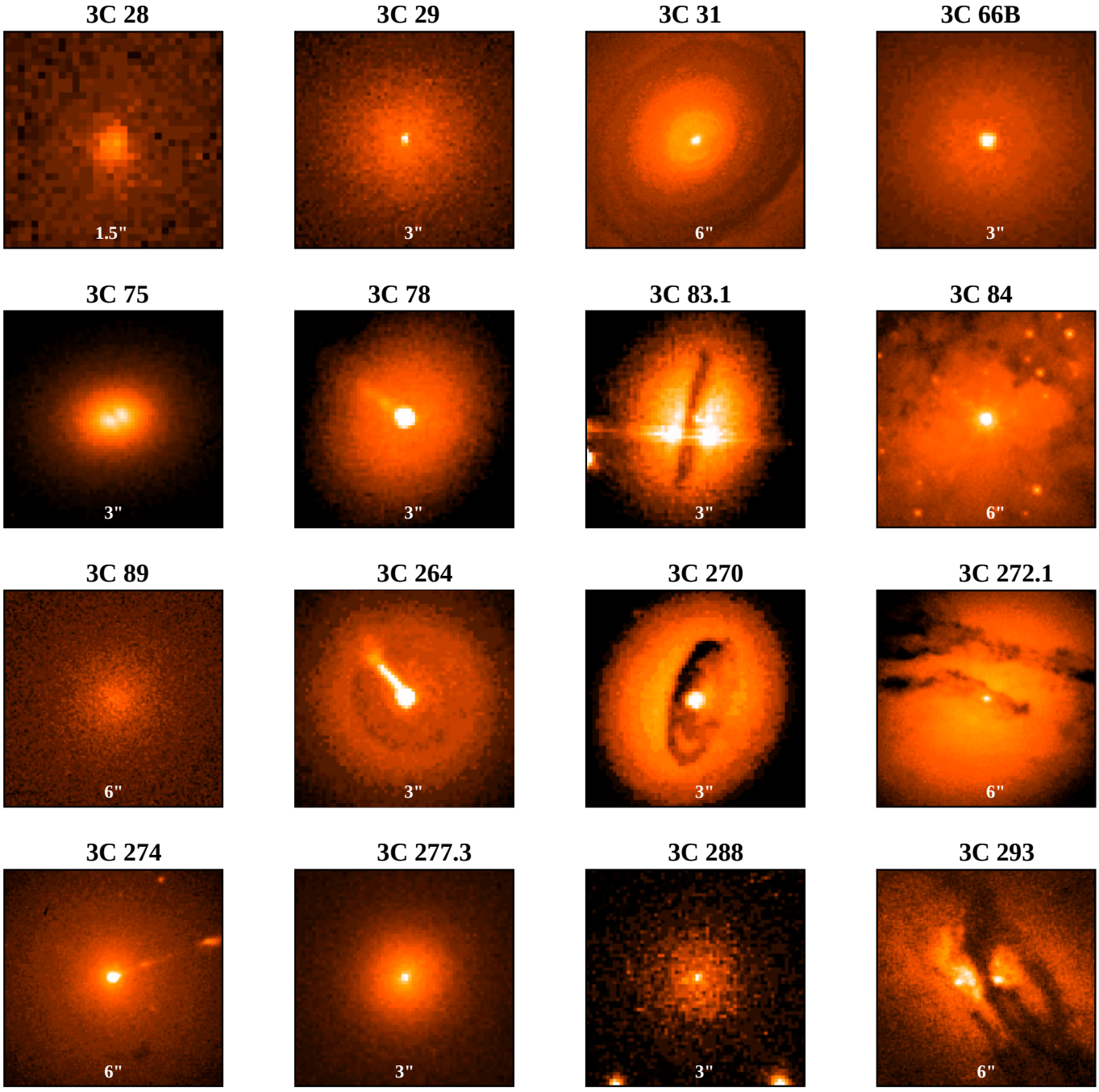

Fig. 1. HST/WFPC2 broad band images of the FR I radio galaxies of the sample (a).

In order to quantify this relation let us consider separately the low and high luminosity sub–samples.

The 18 CCCs associated to the low luminosity sources show a tight correlation between F_o and F_r. Only one point, representing 3C 386, is well separated from the others. We perform a non-weighted least squares fit (excluding 3C 386): the correlation coefficient is $r = 0.88$ which gives a probability that the points are taken from a random distribution of $P = 3.1 \times 10^{-6}$. The dotted lines in Fig. 4 are the fits to the data using each of the two fluxes as independent variables. The best fit is represented by the bisectrix of these two regressions (dashed line) and has a slope of 0.95 ± 0.10. The statistical parameters[1] of the fits are reported in Table 4. A similarly strong correlation ($P = 6.0 \times 10^{-6}$) is present also between radio core and CCC luminosities (Fig. 5). The fact that the correlation is found both in flux and luminosity gives us confidence that it is not induced by either selection effects or a common redshift dependence.

[1] We also performed the linear fit by using a weighted Chi-square method adopting ten per cent errors on both variables and a "robust" least absolute deviation method. The results both in term of probability and linear fits parameters are fully consistent (with even smaller errors) with those reported above.

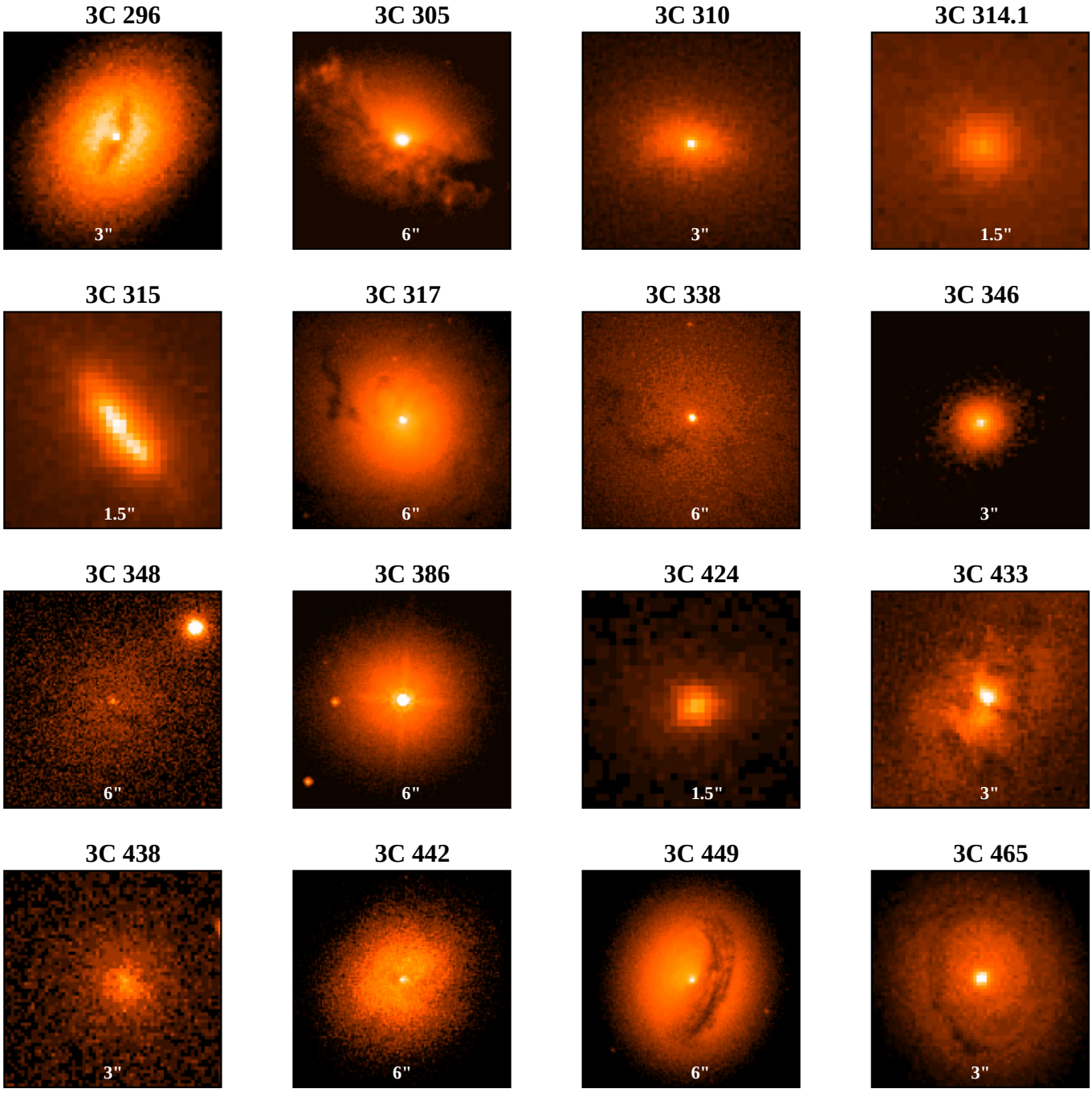

Fig. 2. HST/WFPC2 broad band images of the FR I radio galaxies of the sample (b).

Moreover the 3CR sample has been selected according to the total radio flux at low frequency which is only weakly correlated with the core properties entering in the correlations (e.g. Giovannini et al. 1988).

Let us then consider the case of 3C 386, which we excluded from the statistical analysis. While all points are closely clustered around the linear fit, with a dispersion of only ~ 0.4 dex, 3C 386 deviates by 3 orders of magnitude, clearly indicating that its optical/radio properties differ from the remaining of the sample. This suggestion is strengthened by the presence of a further peculiarity in the optical band of this object, i.e. the detection of a broad Hα line (Simpson et al. 1996), atypical of FR I radio galaxies. In any case, although the inclusion of 3C 386 in the analysis decreases the statistical significance of the correlation to $P = 2.6 \times 10^{-3}$, it would not affect our conclusions.

Turning now to the high luminosity sub-sample, five out of the nine points are upper limits, since no CCC is detected. This prevents us from performing a meaningful statistical analysis. Note, however, that the four detected CCC fluxes lie along the

Table 3. Summary of the CCC photometry

Name	CCC flux, filter 1 erg s^{-1}cm^{-2}Å^{-1}	CCC flux, filter 2 erg s^{-1} cm^{-2} Å^{-1}
3C 028	<3.2 E-19 [a]	
3C 029	(5.8 ± 0.7) E-18 [a]	
3C 031	(1.5 ± 0.4) E-17 [b]	
3C 066B	(4.93 ± 0.07) E-17 [a]	
3C 075	——	
3C 078	(2.38 ± 0.04) E-16 [b]	(3.09 ± 0.05) E-16 [e]
3C 083.1	1.4 E-18:	
3C 084	(1.5 ± 0.3) E-15 [b]	(1.43 ± 0.07) E-15 [g]
3C 089	< 2 E-19	
3C 264	(1.14 ± 0.06) E-16 [c]	(1.54 ± 0.05) E-16 [f]
3C 270	(5.1 ± 0.1) E-18 [c]	(6.0 ± 2.0) E-18 [f]
3C 272.1	(5.9 ± 0.2) E-17 [d]	(4.2 ± 0.1) E-17 [f]
3C 274	(3.9 ± 0.2) E-16 [d]	(6.5 ± 0.2) E-16 [f]
3C 277.3	(1.5 ± 1.2) E-18 [b]	(3.5 ± 1.2) E-18 [e]
3C 288	(7.0 ± 1.0) E-19 [a]	
3C 293	——	
3C 296	(3.4 ± 0.3) E-18 [a]	
3C 305	——	
3C 310	(3.5 ± 0.7) E-18 [a]	
3C 314.1	<9.5 E-19 [a]	
3C 315	——	
3C 317	(9.6 ± 1.0) E-18 [d]	(1.5 ± 0.2) E-17 [e]
3C 338	(1.0 ± 0.1) E-17 [b]	
3C 346	(2.3 ± 0.3) E-17 [a]	
3C 348	(8.0 ± 1.0) E-19 [a]	
3C 386	(1.4 ± 0.1) E-15 [a]	
3C 424	<1.5 E-18 [a]	
3C 433	——	
3C 438	<4.0 E-19 [a]	
3C 442	(9.1 ± 3.3) E-19 [a]	(8.0 ± 2.0) E-19 [f]
3C 449	(1.8 ± 0.1) E-17 [b]	
3C 465	(1.9 ± 0.1) E-17 [b]	

HST filters coding: [a] F702W, [b] F702W line subtr., [c] F791W, [d] F814W, [e] F555W, [f] F547M, [g] F450W

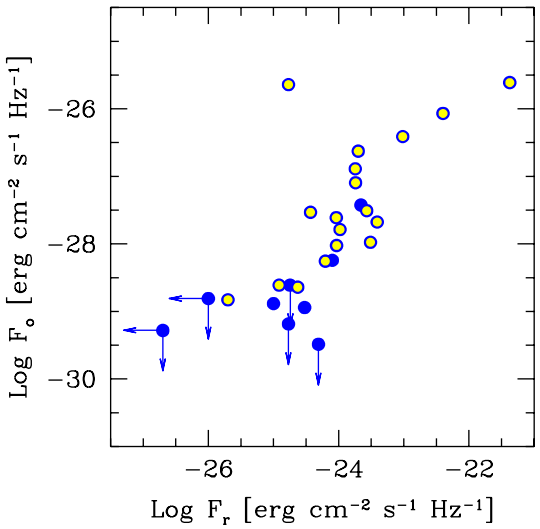

Fig. 3. Optical flux of the CCC versus core radio (5 GHz) flux. Note the clear trend between the two quantities. Only the peculiar object 3C 386 is significantly offset (see text for discussion). Again, different symbols mark sources with total radio luminosity below (open circles) and above (filled circles) $L_{178} = 2 \times 10^{26}$ [W Hz^{-1}].

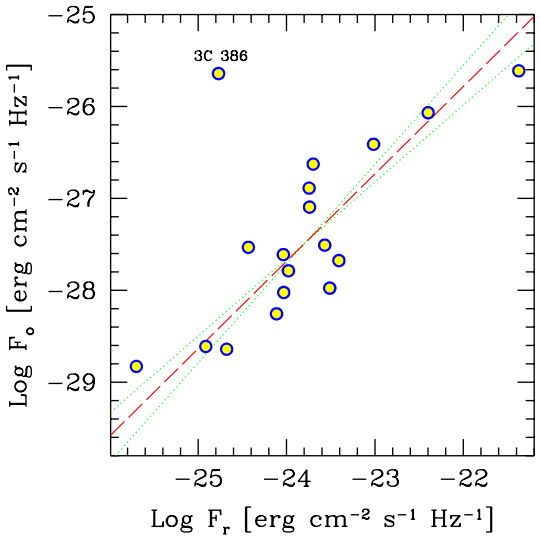

Fig. 4. Optical CCC vs radio core fluxes at 5 GHz for the low power subsample (see text). Dotted lines are the fits to the data using each of the two fluxes as independent variables. Dashed lines represent the best fits. The peculiar object 3C 386 is excluded from the fitting procedure.

same correlation defined by the lower luminosity objects (see Fig. 5).

We conclude that a striking linear correlation is present between the core radio and CCC fluxes (and luminosities): it extends over four orders of magnitude, has an extremely high statistical significance, a small dispersion and a slope consistent with unity. Since the radio core emission is certainly originated as synchrotron radiation the above tight link is a strong suggestion that also the optical CCC emission is produced by the same non–thermal process.

Independent support for this hypothesis comes from considering the spectral information relative to the CCCs, which can be compared with that of sources where synchrotron emission dominates in the optical as well as in the radio band (e.g. blazars, optical jets). First of all, we find that the radio–optical spectral indices of the CCC of our radio galaxies span the range $\alpha_{ro} \sim 0.6$–0.9, similar to those of optical jets (e.g. Sparks et al. 1994) and at the upper end of the spectral indeces of blazars for which $\alpha_{ro} \sim 0.2$–0.9 (e.g. Fossati et al. 1998).

Furthermore, the CCC optical spectral indices (determined however for only five sources) are in the range $\alpha_o \sim 0.7$–1.3, also typical of the synchrotron-emitting sources mentioned above.

5.1. Alternative explanations

Even though synchrotron radiation provides a rather convincing interpretation of the nature of CCCs, in the following we con-

Table 4. Linear fit parameters

r	0.88		
P	3.1×10^{-6}		
F_o vs F_r	$a = 0.84 \pm 0.12$	$b = -7.5 \pm 2.8$	rms = 0.42
F_r vs F_o	$a = 0.92 \pm 0.13$	$b = 1.7 \pm 3.5$	rms = 0.44

Statistical parameters for the correlation between radio core and optical CCC fluxes. The fitted linear relation is of the form $y = ax + b$.

sider and discuss other emission processes usually occurring in the nuclei of active galaxies. We should however note that none of these mechanisms seems to account naturally for the linear correlation between the radio and optical CCC luminosities and even less for its small dispersion, as radio cores are strongly affected by relativistic beaming while in all alternative scenarios the optical emission is essentially quasi–isotropic.

• Nuclear cusps or star clusters: recent work has shown that stellar concentrations are often present in the nuclear regions of elliptical galaxies (e.g. Lauer et al. 1995). However, the CCCs optical spectral slopes are not compatible with the 'red' colors typical of old stellar populations.

• Nuclear starburst: as CCCs are observed in the great majority of the galaxies of our sample, star formation should be maintained continuously for a timescale comparable to the lifetime of the radio sources, i.e. $\sim 10^{7-8}$ yr (Parma et al. 1999). Although some ad hoc mechanisms regulating the star formation rate might exist, this possibility appears implausible.

• Accretion discs: the optical spectral information also contrasts with the emission expected at least in the simplest hypothesis of a Shakura-Sunyaev geometrically thin, optically thick disk, which generally predicts a harder spectral slope ($\alpha \lesssim -0.3$). A softer index is expected only at higher frequencies (UV–soft–X; e.g. Szuszkiewicz et al. 1996). No observational constraints are provided by more complex disc models (e.g. the recently proposed case of low density radiatively inefficient accretion flows, ADAF, Rees et al. 1982; Narayan & Yi 1995; Chen et al. 1997) as they can reproduce widely different spectral slopes in the optical band.

• Emission line region: as already pointed out, although line emission contributes from 5 to 40 per cent, continuum emission provides the bulk of the total CCC flux.

We conclude from this analysis that there is no other likely explanation for the origin of CCCs, except non–thermal synchrotron emission.

6. Discussion

6.1. Implications for unified models

For the first time, thanks to the high spatial resolution of HST, it has been possible to separate the contribution of the host galaxy from the genuine nuclear emission in FR I radio galaxies, which manifests itself as a Central Compact Core.

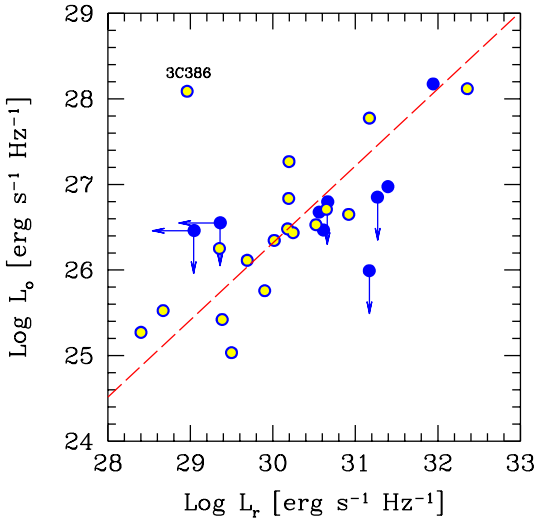

Fig. 5. CCC luminosity versus radio (5 GHz) core luminosity for both the lower (open circles) and higher (filled circles) total radio luminosity. The dashed line is the best fit to the data of the low luminosity subsample, having excluded the peculiar object 3C 386.

CCCs appear to be associated with non–thermal synchrotron emission. Three pieces of evidence also suggest that the CCC radiation is anisotropic due to relativistic beaming:

1. Capetti & Celotti (1999) studied five radio galaxies in which HST images revealed the presence of extended nuclear discs, which appear to be useful indicators of the radio sources orientation. The FR I CCC luminosity shows a suggestive correlation with the orientation of the radio galaxies with respect to the line of sight;
2. Sparks et al. (1995) argued that jets are detected in the optical band only when pointing towards the observer. This would explain why jets with optical counterparts are smaller (they are foreshortened), brighter and one-sided (they are relativistically beamed) with respect to typical radio jets. Five sources of our sample (namely 3C 66B, 3C 78, 3C 264, 3C 274 and 3C 346) indeed show optical jets and these very same objects clearly stand out for being among the brightest CCC of their respective subsamples (see Fig. 6 where we report the CCC luminosity versus the total radio power). Sources with optical jets are also the only FR I galaxies detected in UV HST observations (Zirbel & Baum 1998);
3. as noted above, the radio core emission is certainly beamed and the corresponding orientation dependence is reflected in the large spread found when comparing the core to extended (quasi–isotropic) radio luminosities (Giovannini et al. 1988). Therefore if the optical emission were isotropic the F_o vs F_r correlation would show at least a similarly large scatter.

The beamed synchrotron scenario which emerges for the origin of the CCC is therefore strong evidence in favour of the idea that FR I are the misoriented counterparts of BL Lacs. The large spread (3 orders of magnitude) in CCC luminosity among objects of similar extended properties (see Fig. 6) can be ascribed

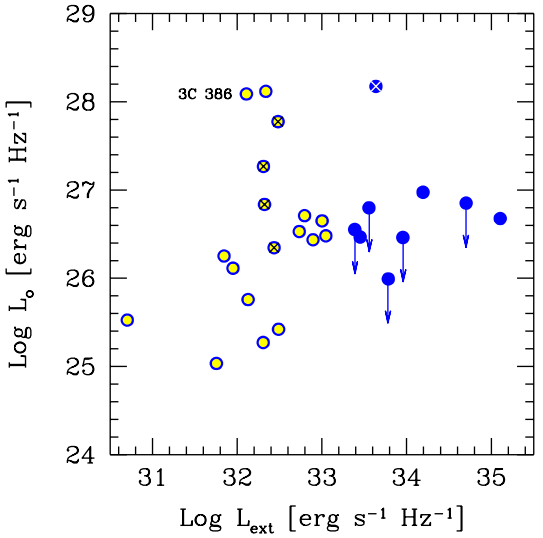

Fig. 6. Optical CCC luminosity versus total radio luminosity. Again, different symbols mark sources with total radio luminosity below (open circles) and above (filled circles) $L_{178} = 2 \times 10^{26}$ [W Hz^{-1}]. Crossed symbols are for galaxies with known optical jets.

to different orientations. An extensive and quantitative analysis of this issue and of the relationship between FR I and BL Lacs in the light of these results will be presented in a forthcoming paper (Chiaberge et al., in prep).

6.2. Are there obscuring tori in FR I?

The observation of optical synchrotron emission has important consequences on the role/geometry of absorption structures in the nuclear regions of such objects. A very important result of our analysis is in fact the high fraction of galaxies in which the central source has been detected.

Limiting ourselves, for the moment, to the low luminosity subsample, we found a CCC in 85% of the objects. The sources in which we do not detect it (namely 3C 75, 3C 293 and 3C 305) are three out of the four cases in which the center of the galaxy is affected by obscuration from a large scale dust structure (the fourth galaxy is 3C 272.1 whose CCC, although reddened, shines through the dust lane). In order to estimate the optical depth of obscuring material in these sources, we derived their expected optical flux from the CCC vs radio core flux correlation. We found that an extinction of only a few magnitudes ($A_V \lesssim 6$ mag, corresponding to a column density of $N_H \lesssim 1.2\ 10^{22}$ cm^{-2}) is sufficient to hide the CCC optical emission. Therefore, even in these three cases the presence of an optically (Thomson) thick structure is not required (although it cannot be ruled out) and the CCC emission might be simply obscured by the foreground dust. Infrared observations can address this issue.

The behaviour of the 11 sources with higher total radio luminosity is probably different and certainly more complex:
– four of them have CCC fluxes and luminosities consistent with the correlations found for lower power FR I, and would simply lie on the high luminosity part of the radio–optical correlation (see Fig. 5)
– two of them show complex (possibly absorbed) nuclei;
– in the last five objects no unresolved component is detected (upper limits in Figs. 3, 6, 5; see also Sect. 4). The upper limits derived could be in general agreement with the F_o vs F_r CCC correlation, except possibly in the case of 3C 89 (the lowest point in Fig. 3).

The smaller number of CCC found could be simply due to the fact that this subsample is on average at higher redshift. Clearly, we cannot exclude the alternative possibility, i.e. that these sources are indeed obscured, which might indicate that the degree of obscuration increases with the source power (a crucial test here is the inclusion in the sample of high luminosity FR II radio galaxies; Chiaberge et al., submitted).

The detection of CCCs indicates that we have a direct view of the innermost nuclear regions of FR I. Limits on the extension of CCC are implied by the variability of the nucleus of M 87 on time scales of two months (Tsvetanov et al. 1998). Furthermore, since the optical emission in relativistic jets is likely to be produced co-spatially or even closer to the black hole with respect to the radio emission, we can infer a further constraint on the CCC extension from VLBI observations. These in fact show that most of the radio emission comes from a source unresolved at mas resolution which can be as small as 0.01 pc, i.e. only ~ 100 Schwarzschild radii for a $\sim 10^9$ M$_\odot$ black hole (e.g. Junor & Biretta 1995).

It therefore appears that a “standard”, pc scale, geometrically thick torus is not present in low luminosity radio galaxies. Any absorbing material must be distributed in a geometrically thin structure (our CCC detection rate implies a thickness over size ratio $\lesssim 0.15$) or thick tori are present only in a minority of FR I. This result is particularly intriguing since dusty nuclear discs on kpc scales have been discovered in several FR I and they indeed are geometrically thin (Jaffe et al. 1996). In this sense, the lack of broad emission lines in FR I cannot be accounted for by obscuration.

6.3. Limits on thermal disc emission and AGN efficiency

Except for blazars, whose overall spectral energy distributions are almost always dominated by the non–thermal emission from a relativistic jet, the nuclear emission of AGNs from the optical to the soft-X band is generally interpreted as thermal emission from accreting material. Conversely, we find that in FR I a non–thermal synchrotron component dominates the emission in all sources. In fact, a sufficiently bright isotropic optical component would produce a flattening in the radio/optical CCC correlation, due to the presence of an additional source of optical flux (with no radio counterpart), which we do not observe (see Figs. 4 and 5). This is surprising if one considers that, in a complete sample, a substantial fraction of the objects are observed at large angles from the line of sight and thus the emission from their jets is expected to be strongly de-beamed, favouring the detection of any isotropic (disc) emission.

The CCC fluxes thus set upper limits to the disc emission, which in turn imply extremely low radiative efficiency of the accretion process. Note, in fact, that the observed CCC emission corresponds to $\lesssim 10^{-7}$–10^{-5} of the Eddington luminosity of a $10^9 M_\odot$ black hole, which appears to be typical for these radio galaxies. While these values argue against the presence of a radiatively efficient accretion phase, they are still compatible with the expected radiative cooling rate of low density and high temperature accreting plasma in which the electron–ion coupling is ineffective and most of the thermal energy is thus advected inwards and not radiated (Rees et al. 1982; also ADAF, e.g. Narayan & Yi 1995, Chen et al. 1997 and ADIOS, Blandford & Begelman 1999). This latter possibility has been indeed proposed to account for the paucity of emission in radio galaxies harbouring supermassive black holes (Fabian & Rees 1995). The HST observations of CCC set consistent but independent constraints relative to the optical emission in these systems.

This low efficiency in producing thermal emission might also account for the lack of broad lines in FR I spectra, which could be attributed just to the lack of those ionizing photons which, in the other classes of active nuclei, illuminate the dense clouds forming the Broad Line Region. Indeed Zirbel et al. (1995) have suggested the possibility that FR I sources produce far less UV radiation than FR II on the basis of the comparison between emission line and radio luminosities of radio galaxies. Intriguingly, the only object in which a broad line has been detected is 3C 386, whose CCC presents a much larger optical luminosity with respect to the sources with similar radio core power, possibly indicative of a thermal contribution.

7. Summary and conclusions

HST images of a complete sample of 33 FR I radio galaxies belonging to the 3CR catalogue have revealed that an unresolved nuclear source (Central Compact Core, CCC) is present in the great majority of these objects.

The CCC emission is found to be strongly connected with the radio core emission and anisotropic. We propose that the CCC emission can be identified with optical synchrotron radiation produced in the inner regions of a relativistic jet. Support for this possibility comes also from spectral information. These results are qualitatively consistent with the unifying model in which FR I radio galaxies are misoriented BL Lac objects.

The identification of the CCC radiation with misoriented BL Lac emission opens the possibility of studying this class of AGNs from a different line of sight. This can be particularly useful in understanding the jet structure and the level of the activity occurring near the central object whose emission in blazars is swamped by the highly beamed component. Further information on the nature of CCC can be inferred by simultaneous studies of radio cores and CCC optical variability which could establish whether their emission is indeed produced in the same region.

The detection of CCC indicates that we have a direct view of the innermost regions of the AGN ($\lesssim 100 R_S$). If we restrict the analysis to objects with a total radio power of $< 2 \times 10^{26}$ W Hz^{-1}, a CCC is found in all galaxies except three, where absorption from extended dust structures clearly plays a role. This casts serious doubts on the presence of obscuring thick tori in FR I as a whole.

Given the dominance of non-thermal emission, the CCC luminosity represents a firm upper limit to any thermal component, which translates into an optical luminosity of only $\lesssim 10^{-5} - 10^{-7}$ times the Eddington one (for a $10^9 M_\odot$ black hole). This limit on the radiative output of accreting matter is independent but consistent with those inferred in X–rays for large elliptical galaxies, thus suggesting that accretion might take place in a low efficiency radiative regime (Fabian & Rees 1995).

The picture which emerges is that the innermost structure of FR I radio galaxies differs in many crucial aspects from that of the other classes of AGN; they lack the substantial BLR, tori and thermal disc emission, which are usually associated with active nuclei. Similar studies of higher luminosity radio galaxies will be clearly crucial to determine if either a continuity between low an high luminosity sources exists or, alternatively, they represent substantially different manifestations of the accretion process onto a supermassive black hole.

Acknowledgements. The authors thank G. Bodo and E. Trussoni for useful comments on the manuscript and acknowledge the Italian MURST for financial support.

This research has made use of the NASA/IPAC Extragalactic Database (NED) which is operated by the Jet Propulsion Laboratory, California Institute of Technology, under contract with the National Aeronautics and Space Administration.

References

Antonucci R.R.J., Miller J.S., 1985, ApJ 297, 621
Barthel P.D., 1989, ApJ 336, 606
Biretta J.A., Burrows C.J., Holtzman J.A., et al., 1995, In: Biretta J.A. (ed.) Wide Field and Planetary Camera 2 Instrument handbook. STScI, Baltimore
Black A.R.S., Baum S.A., Leahy J.P., et al., 1992, MNRAS 256, 186
Blandford R.D., Begelman M.C., 1999, MNRAS 303, L1
Bower G.A., Green R.F., Danks A., et al., 1998, ApJ 492, L111
Braatz J.A., Wilson A.S., Henkel C., 1996, ApJS 106, 51
Capetti A., Celotti A., 1999, MNRAS 304, 434
Capetti A., Fanti R., Parma P., 1995, A&A 300, 643
Chen X., Abramowicz M.A., Lasota J.-P., 1997, ApJ 476, 61
Colina L., De Juan L., 1995, ApJ 448, 548
De Koff S., Baum S., Sparks W.B., et al., 1995, BAAS 187, 1202
De Koff S., Baum S.A., Sparks W.B., et al., 1996, ApJS 107, 621
Fabian A.C., Rees M.J., 1995, MNRAS 277, L55
Fanaroff B.L., Riley J.M., 1974, MNRAS 167, 31
Ferrarese L., Ford H., Jaffe W., 1996, ApJ 470, 444
Ford H.C., Harms R.J., Tsvetanov Z.I., et al., 1994, ApJ 435, L27
Fossati G., Maraschi L., Celotti A., Comastri A., Ghisellini G., 1998, MNRAS 299, 433
Giovannini G., Feretti L., Gregorini L., Parma P., 1988, A&A 199, 73
Gonzales-Serrano I., Carballo R., Perez-Fournon I., 1993, AJ 105, 1710
Harms R.J., Ford H.C., Tsvetanov Z.I., et al., 1994, ApJ 435, L35
Henkel C., Wang Y.P., Falcke H., Wilson A.S., Braatz J.A., 1998, A&A 335, 463

Jaffe W., Ford H.C., Ferrarese L., Van den Bosh F., Ó Connell R.W., 1993, Nat 364, 213
Jaffe W., Ford H., Ferrarese L., Van den Bosh F., Ó Connell R.W., 1996, ApJ 460, 214
Junor W., Biretta J.A., 1995, AJ 109, 506
Laing R.A., Riley J.M., Longair M.S., 1983, MNRAS 204, 151
Lauer T.R., Ajhar E.A., Byun Y.-I., et al., 1995, AJ 110, 2622
Leahy J.P., Perley R.A., 1991, AJ 102, 537
Macchetto F., Albrecht R., Barbieri C., et al., 1991, ApJ 373, L55
Macchetto F., Marconi A., Axon D.J., et al., 1997, ApJ 489, 579
Martel A.R., Baum S.A., Sparks W.B., et al., 1999, ApJS 122, 81
Miyoshi M., Moran J., Herrnstein J., Greenhill L., et al., 1995, Nat 373, 127
Morganti R., Ulrich M.H., Tadhunter C.N., 1992, MNRAS 254, 546
Morganti R., Killeen N.E.B., Tadhunter C.N., 1993, MNRAS 263, 1023
Narayan R., Yi I., 1995, ApJ 444, 231
Parma P., De Ruiter H.R., Fanti C., Fanti R., Morganti R., 1987, A&A 181, 244
Parma P., Murgia M., Morganti R., et al., 1999, A&A 344, 7
Rees M.J., Phinney E.S., Begelman M.C., Blandford R., 1982, Nat 295, 17
Riley J.M., Pooley G.G., 1975, Mem. R. Astron. Soc. 80, 105
Simpson C., Ward M., Clements D.L., Rawlings S., 1996, MNRAS 281, 509
Sparks W.B., Biretta J.A., Macchetto F., 1994, ApJS 90, 909
Sparks W.B., Golombek D., Baum S.A., et al., 1995, ApJ 450, L55
Spinrad H., Djorgovski S., Marr J., Aguilar L., 1985, PASP 97, 932
Strom R.G., Willis A.G., Wilson A.S., 1978, A&A 68, 367
Szuszkiewicz E., Malkan M.A., Abramowicz M.A., 1996, ApJ 458, 474
Taylor G.B., Vermeulen R.C., Readhead A.C.S., et al., 1996, ApJS 107, 37
Tsvetanov Z.I., Hartig G.F., Ford H.C., et al., 1998, ApJ 493, L83
Urry C.M., Padovani P., 1995, PASP 107, 803
Van der Marel R.P., Van den Bosch F.C. 1998, AJ 116, 2220
Zirbel E.L., 1997, ApJ 476, 489
Zirbel E.L., Baum S.A., 1995, ApJ 448, 521
Zirbel E.L., Baum S.A., 1998, ApJS 114, 177
Zirbel E.L., Baum S.A., O'Dea C.P., 1995, ApJ 451, 88